European ECOSTRESS Hub
Algorithm Theoretical Basis Document Land Surface Temperature

Reference: EEH-D5-ATBDET

ESA Contract No. 4000129873/20/I-NS

Prepared by	Tian Hu, Kaniska Mallick, Martin Schlerf, Patrik Hitzelberger and Yoanne Didry (LIST)
Reference	EEH-D5-ATBDET
Issue	1
Revision	0
Date of Issue	2021-05-21
Status	**Final Approved Version**

CHANGE LOG

Issue	Revision	Date	Author	Comment
1	0	2021-05-21	Hu, Mallick, Schlerf, Hitzelberger, Didry	Final version

Contents

Abstract

Evapotranspiration (ET) is an important component of the terrestrial hydrological cycle and land-atmosphere interaction. It relates closely to the ecosystem carbon assimilation, and mass and energy exchange at the surface-atmosphere interface (Chen and Liu 2020), thus playing an important role in climate and meteorology, ecosystem dynamics, and nutrient biogeochemistry (Mallick et al. 2016). Thermal infrared (TIR) remote sensing, due to its close connection to the surface radiation budget and energy balance, has been widely used in global ET retrieval. Land surface temperature (LST) obtained from TIR remote sensing is immensely sensitive to evaporative cooling and surface water content (Anderson et al., 2011; Kustas and Anderson, 2009). It provides direct information on the land surface moisture status and surface energy balance partitioning (Kustas and Anderson, 2009; Mallick et al., 2014; Chen and Liu 2020), and sets the lower boundary conditions for the transfer of latent and sensible heat through the soil-vegetation-atmosphere continuum. It offers a diagnostic ET assessment tool without the additional information on precipitation or soil pedotransfer functions as commonly required in hydrological models (Anderson et al., 2011; Anderson and Kustas, 2008). Normally, moisture deficiency in the vegetation root zone leads to the closure of stomata, a reduction in transpiration and elevated canopy temperatures (Anderson et al., 2011; Anderson & Kustas, 2008). In addition, the depletion of water from the soil surface layer leads to the rapid heating of the soil surface and results in reduced evaporation (Anderson et al., 2011; Kustas and Anderson, 2009).

Recently there has been a rapid progress in the model development for generating spatially distributed evapotranspiration using remotely sensed LST data. The LST-based ET models can be broadly divided into two categories. All these models use the surface energy balance (SEB) equation. Most models calculate the sensible heat flux (H) by solving the aerodynamic conductance for heat (g_a) and estimate latent heat flux (λE) indirectly as a residual of the surface energy balance, such as the Two Source Energy Balance (TSEB) model, the Surface Energy Balance System (SEBS) model and the Soil Plant Atmosphere and

Remote Sensing Evapotranspiration (SPARSE) model. In the second category, LST is integrated into the Penman-Monteith formulation to calculate *LE* and *H* directly, and the Surface Temperature Initiated Closure (STIC) model is the only model until now which adopts such approach. The ECOsystem Spaceborne Thermal Radiometer Experiment on Space Station (ECOSTRESS) mission provides LST retrievals at global scale with a high spatial resolution (~70 m) and multiple revisits in a day, which provides an unprecedented opportunity to investigate the diurnal change of surface water availability and quantify water demand in the agriculture intensive regions. In the European ECOSTRESS Hub (EEH), three different models, i.e. STIC, SEBS, and TSEB, are adopted, covering both categories of LST-based ET models. The selection also encompasses both one-source model (STIC and SEBS) and two-source model (TSEB). This ATBD will elaborate on the application of these three models to ECOSTRESS ET retrieving driven by the corresponding LST estimates.

1. Introduction

Evapotranspiration (ET), consisting of evaporation (E) from soil and wet vegetation surfaces and transpiration (T) from plant leaves, is the main source for water loss from the terrestrial ecosystems. Due to the complex biophysical controls on E and T and highly heterogeneous vegetation covers and soil properties, accurate ET estimation remains a difficult task (Chen and Liu 2020; Fisher et al. 2020; Mallick et al. 2015; Mallick et al. 2018a; Mallick et al. 2016). Multiple models have been developed to retrieve ET using remote sensing observations, including the temperature-based and vapor pressure-based models. By employing the thermal infrared (TIR) imager prototype HyspIRI Thermal Infrared Radiometer (PHyTIR) onboard the International Space Station (ISS), ECOSTRESS (ECOsystem Spaceborne Thermal Radiometer Experiment on Space Station) provides observations in five spectral bands between 8 and 12.5 μm at a spatial resolution of 38 m by 69 m with multiple revisits in a day, from which land surface temperature (LST) can be retrieved. Taking advantage of the ECOSTRESS Level-2 LST retrievals, the LST-based ET models are focused on in the European ECOSTRESS Hub (referred to as EEH here after).

Currently, most temperature-based ET models calculate ET as a residual of the surface energy balance after estimating the sensible heat flux or estimate the evaporative fraction first and derive ET from the available energy, including the Two Source Energy Balance (TSEB) model (Norman et al. 1995) and the Surface Energy Balance System (SEBS) model (Su 2002). These models can be broadly characterized as one-source and two-source models based on the conceptualization of the land surface. In the one-source model, the vegetated surface is regarded as a ‘big leaf’ and evaporating front is assumed to be at the source/sink height, which is in the immediate vicinity of the surface level. Whereas, the two-source model assumes the vegetated surface to consist of the soil and vegetation components, and the energy fluxes are partitioned between these two components. Different from these models, the Surface Temperature Initiated Closure (STIC) model, being as one-source model, retrieves ET directly by introducing temperature retrievals into the Penman-

Monteith (PM) formulation and combining the advection-aridity hypothesis and the Shuttleworth-Wallace model (Mallick et al. 2016).

To encompass models with different complexities and conceptualization approaches, the STIC, TSEB and SEBS models are used in the EEH-ET module. This ATBD will elaborate on these three ET models and their applications to ECOSTRESS LST estimates.

2. Theory and basis

Evapotranspiration is intrinsically associated with the surface energy balance equation, which is based on the partitioning of net available energy into sensible and latent heal fluxes. The surface energy balance (SEB, hereafter) equation is written as follows:

$$R_N = \lambda E + H + G \quad (2.1)$$

where H and λE are sensible and latent heat fluxes (W m^{-2}), respectively, G is the ground heat conduction flux. The segregation of net available energy (the difference between net radiation R_N and ground heat flux G) in these two different convective fluxes depends on the land surface moisture status, atmospheric conditions in the boundary layer, and biophysical control of vegetation (Mallick et al. 2014; Mallick et al. 2018a; Mallick et al. 2018b).

2.1. Surface radiation budget and energy balance

The surface net radiation (R_N) is calculated as follows:

$$R_N = (1 - \alpha_{alb})R_s + \varepsilon_{bb}R_{lwd} - \varepsilon_{bb}\sigma {T_s}^4 \quad (2.2)$$

where α_{alb} is the broadband surface albedo, R_s is the downwelling shortwave insolation, ε_{bb} is the broadband surface emissivity in the thermal infrared domain, R_{lwd} is the atmospheric longwave downward radiation, σ is the Stefan-Boltzmann constant (5.67 x 10^{-8} W m^{-2} K^{-4}), T_s is the surface radiometric temperature.

2.2. Basic formulation for heat flux estimation

Based on the flux gradient theory, sensible and latent heat fluxes can be calculated as follows:

$$H = \rho c_p \frac{T_0 - T_a}{r_a} \quad (2.3)$$

$$\lambda E = \frac{\rho c_p}{\gamma} \frac{{e_0}^* - e_a}{r_a + r_s} \quad (2.4)$$

where ρ is the density of air (kg m^{-3}), c_p is the specific heat of air at constant pressure (MJ kg^{-1} K^{-1}), γ is the psychrometric constant (hPa K^{-1}), T_0 and T_a are aerodynamic temperature (i.e. air temperature at the source/sink height where wind speed is zero) and air temperature at the reference height, ${e_0}^*$ and e_a are the saturation vapour pressure at T_0 and air vapour pressure,

r_a and r_s are the aerodynamic resistance and surface resistance, respectively. The roughness lengths for heat and water vapour transfer are assumed to be the same in the above equations.

Denoting the slope of the saturation vapour pressure and temperature curve (the Clausius-Clapeyron relationship) as

$$\Delta = \frac{de^*(T)}{dT} \tag{2.5}$$

and taking the first-order Taylor's approximation at air temperature, expressed as

$$\Delta = \frac{{e_a}^* - {e_0}^*}{T_a - T_0} \tag{2.6}$$

the Penman-Monteith (PM) formulation (Monteith 1965) can be obtained by combining Equations 2.1 and 2.2,

$$\lambda E = \frac{\Delta\phi + \rho c_p g_a D_a}{\Delta + \gamma(1 + \frac{g_a}{g_s})} \tag{2.7}$$

where ϕ is the net available energy ($R_N - G$), D_a is the vapour pressure deficit (VPD) of the air at the reference height, g_a and g_s are the aerodynamic conductance and surface conductance, respectively, calculated as the reciprocal of the corresponding resistance mentioned previously. In the PM model, the integrated control from the available energy to support the demand on the latent heat of vaporization and the atmospheric drying power (i.e. VPD), as well as the control from aerodynamic conductance (depending on wind speed, surface roughness, vegetation height and atmospheric stability) and surface conductance (depending on surface wetness, vegetation structure and plant physiology) are integrated. When the surface resistance approaches 0, then the PM equation becomes the Penman equation (Penman 1948).

By neglecting the adiabatic term in the Penman equation, Priestley and Taylor (1972) proposed an empirical adjustment of the equilibrium evaporation expression as follows

$$\lambda E_{PT} = \alpha \frac{\Delta\phi}{\Delta + \gamma} \tag{2.8}$$

where α is the compensation factor introduced due to the simplification. For a large saturated landscape with minimum advection, the best estimate of α was found to be 1.26.

2.3. Conceptualization of the land surface

In the ET models, the land surface is mainly described from two different perspectives, either as a 'big leaf' or as individual soil and vegetation components, i.e. the one-source and two-source models. In most of the LST-based ET models, λE is calculated as the residual of the net available energy after obtaining H. Only few calculate λE directly.

2.3.1. One-source model

In the one-source models (OSM, hereafter), the land surface is regarded as a 'big leaf' overlaying the ground and no distinction is made to separate soil and vegetation. Heat transfer from the vegetated surface to the atmosphere occurs at a representative height defined as the zero-displacement height plus a roughness length for heat transfer (d_0 + z_{0h}). The bulk aerodynamic resistance is a composite of the soil and vegetation resistors.

2.3.2. Two-source model

In the two-source models (TSM, hereafter), the land surface is discretised into soil and vegetation components and convective fluxes are estimates from the individual soil/vegetation component. Two different resistance networks are conceptualized in the TSMs: parallel resistance network and more complex series network. In the parallel resistance network, soil and vegetation components interact with the lower atmosphere boundary layer in parallel. The soil and canopy resistance components are hypothesized to operate independently and without any interaction between them. In the series resistance network, heat transfer from soil and vegetation components are first assembled at a representative height. Then, the heat is transferred from the representative height to the air.

In this ATBD, we will describe the fundamental equations of three structurally different SEB models that are used for the ET product development in the EEH. The three models are STIC (Surface Temperature Initiated Closure), SEBS (Surface Energy Balance System) and TSEB (Two-source Energy Balance Model). The fundamental differences among these three models are the structures. STIC is a one-source non-parametric model, SEBS is an OSM where the aerodynamic conductance is parameterized based on empirical approximations of

surface roughness and atmospheric stability variables. On the contrary, TSEB is a TSM which uses bottom-up approximation to estimate the resistances from soil and canopy component while simultaneously partition LST into soil and canopy temperatures, respectively. For estimating the resistance components, TSEB also uses empirical approaches to estimate surface roughness-related parameters for correcting the atmospheric stability.

3. Surface Temperature Initiated Closure (STIC) model

STIC model was first proposed by Mallick et al. (2014). STIC is based on integration of radiometric temperature into the PM formulation to find analytical solution of the two critical conductances. In order to do so, STIC combines an LST-driven water stress index with aerodynamic equations of *H* and λE and a modified complementary relationship advection-aridity hypothesis (Mallick et al. 2015). The latest version of STIC (Mallick et al. 2016) combines the Shuttleworth-Wallace sparse canopy formulation model with the PM big-leaf model to calculate the vapour pressure at the source/sink height (Shuttleworth and Wallace 1985). The diagram of the STIC model is shown in Figure 3.1 below.

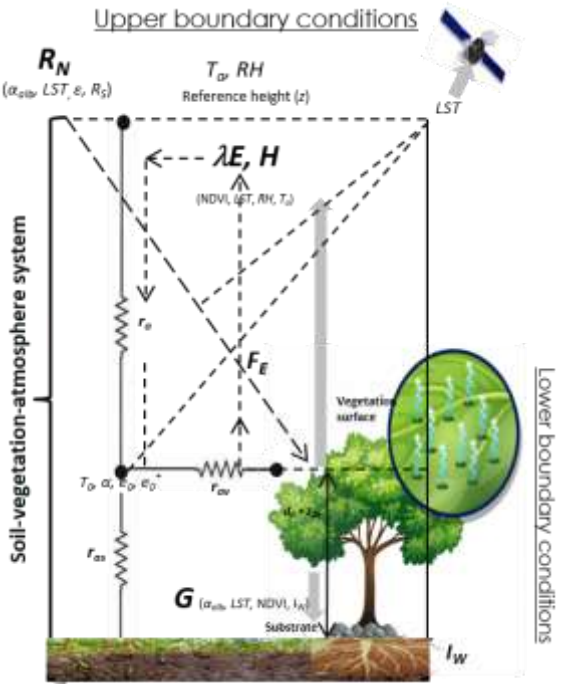

Figure 3.1. Diagram of the STIC model. T_0, e_0 and e_0^* are the aerodynamic temperature, vapour pressure and saturation vapour pressure at the source/sink height. F_E is the evaporative fraction.

3.1. Derivation of state equations

Neglecting horizontal advection and energy storage, the surface energy balance equation is written as follows:

$$\phi = \lambda E + H. \tag{3.1}$$

In the model, *H* is controlled by a single aerodynamic resistance ($r_A = 1/g_A$); λE is controlled by two resistances in series, the surface resistance ($r_C = 1/g_C$) and the aerodynamic resistance

(r_A = 1/ g_A) to vapour transfer. For simplicity, it is implicitly assumed that the aerodynamic resistance of water vapour and heat are equal, and both the fluxes are transported from the same level from near surface to the atmosphere. The sensible and latent heat fluxes can be expressed in the form of aerodynamic transfer equations as follows:

$$H = \rho c_p g_A (T_0 - T_A) \tag{3.2}$$

$$\lambda E = \frac{\rho c_p}{\gamma} g_A (e_0 - e_A) = \frac{\rho c_p}{\gamma} g_C ({e_0}^* - e_0) \tag{3.3}$$

where T_0 and e_0 are the air temperature and vapour pressure at the source/sink height (i.e. aerodynamic temperature and vapour pressure), ${e_0}^*$ is the saturation vapour pressure at T_0, e_A is the atmosphere vapour pressure. They represent the temperature and vapour pressure of the quasi-laminar boundary layer in the intermediate vicinity of the surface level. T_0 can be obtained by extrapolating the logarithmic profile of T_A down to the source/sink height.

Combining equations (3.1 - 3.3), the aerodynamic conductance can be obtained as follows:

$$g_A = \frac{\phi}{\rho c_p \left[(T_0 - T_A) + \frac{e_0 - e_A}{\gamma} \right]}. \tag{3.4}$$

By combing equations 3.3 and 3.4 and solving g_C, the canopy conductance can be expressed as follows:

$$g_C = g_A \frac{e_0 - e_A}{{e_0}^* - e_0}. \tag{3.5}$$

While deriving the expressions for g_A and g_C, two more unknow variables are introduced (e_0 and T_0), thus two more equations are required to close the system of equations.

An expression for T_0 is derived from the Bowen ratio (β) and evaporative fraction (F_E) equations:

$$\beta = \frac{1 - F_E}{F_E} = \frac{\gamma (T_0 - T_A)}{e_0 - e_A} \tag{3.6}$$

$$T_0 = T_A + \left(\frac{e_0 - e_A}{\gamma} \right) \left(\frac{1 - F_E}{F_E} \right). \tag{3.7}$$

This expression for T_0 introduces another new variable F_E, i.e. evaporative fraction. Therefore, one more equation that describes the dependence of F_E on the conductance is needed. In

order to express F_E in terms of g_A and g_C, the advection-aridity (AA) hypothesis expression (Brutsaert and Stricker 1979) with a modification by Mallick et al. (2015) is adopted.

The AA hypothesis is based on a complementary connection between the potential evaporation (E^*), sensible heat flux (H) and evapotranspiration (E) and leads to an assumed link between g_A and T_0. However, the effects of surface moisture (or water stress) were not explicit in the AA equation. Mallick et al. (2015) implemented a water stress constraint in the AA hypothesis which deriving a state equation of F_E, which is expressed as follows:

$$F_E = \frac{2\alpha s}{2s + 2\gamma + \gamma \frac{g_A}{g_C}(1 + M)} \tag{3.8}$$

where s is the slope of saturation vapour pressure versus temperature curve estimated at T_A, M is the surface moisture availability (0 - 1), which is estimated from LST. From eq. (3.4, 3.5, 3.7 and 3.8), there are 4 equations and 7 unknowns. Therefore, algebraic closure is not possible from these equations and therefore, iterative solution was adopted to estimate the three additional unknown variables (e_0^*, e_0, and α). A flow diagram of STIC is presented in Fig. 3.2 below.

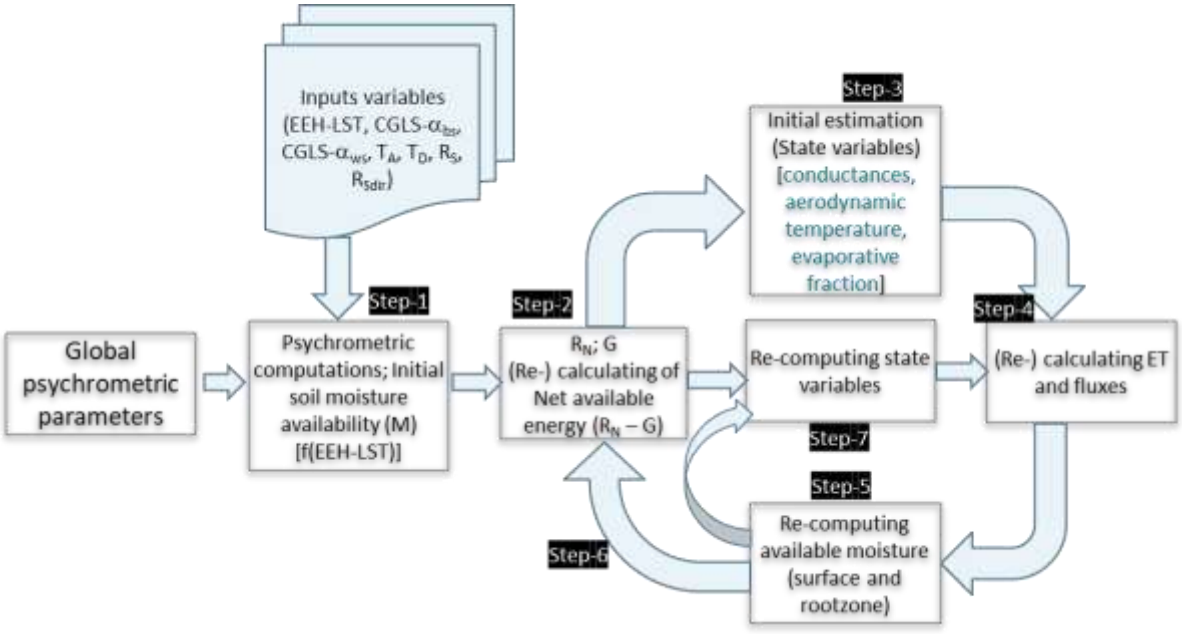

Figure 3.2. An overview of the computational flow for estimating conductances, evaporative fraction, aerodynamic temperature and SEB fluxes in STIC.

3.2. Iterative solution of e_0^*, e_0, α and M in STIC

By inverting the aerodynamic transfer equation of λE, e_0^* can be expressed as

$$e_0^* = e_A + \frac{\gamma \lambda E (g_A + g_C)}{\rho c_p g_A g_C}. \tag{3.9}$$

Following Shuttleworth and Wallace (1985), the vapour pressure deficit ($D_0 = e_0^* - e_0$) and vapour pressure (e_0) at the source/sink height are expressed as follows:

$$D_0 = D_A + \frac{s\phi - (s+\gamma)\lambda E}{\rho c_p g_A} \tag{3.10}$$

$$e_0 = e_0^* - D_0. \tag{3.11}$$

A physical equation of α is derived by expressing the evaporative fraction (F_E) as a function of the aerodynamic equation of H and λE as follows:

$$F_E = \frac{\lambda E}{H + \lambda E} \tag{3.12}$$

$$F_E = \frac{\frac{\rho c_p}{\gamma}\frac{g_A g_C}{g_A + g_C}(e_0^* - e_A)}{\rho c_p g_A (T_0 - T_A) + \frac{\rho c_p}{\gamma}\frac{g_A g_C}{g_A + g_C}(e_0^* - e_A)} \tag{3.13}$$

$$F_E = \frac{g_C (e_0^* - e_A)}{\gamma (T_0 - T_A)(g_A + g_C) + g_C (e_0^* - e_A)}. \tag{3.14}$$

Combining Equations 3.8 and 3.14, we can derive a physical equation of α as

$$\alpha = \frac{\left[2s + 2\gamma + \gamma \frac{g_A}{g_C}(1+M)\right] g_C (e_0^* - e_A)}{2s[\gamma (T_0 - T_A)(g_A + g_C) + g_C (e_0^* - e_A)]}. \tag{3.15}$$

An initial estimate of M is obtained according to the method detailed in Venturini et al. (2008), where M is expressed as the ratio of the vapour pressure difference to the vapour pressure deficit between the surface and atmosphere as follows:

$$M = \frac{e_0 - e_A}{e_0^* - e_A} = \frac{e_0 - e_A}{k(e_S^* - e_A)} = \frac{s_1 (T_{0D} - T_D)}{k s_2 (T_R - T_D)} \tag{3.16}$$

where T_{0D} is the dew-point temperature at source/sink height and T_D is the air dew-point temperature, T_R is the radiometric surface temperature, s_1 and s_2 are the psychrometric slopes of the saturation vapour pressure and temperature between the (T_{0D} - T_D) vs. (e_0 - e_A) and (T_R - T_D) vs. (e_s^* - e_A), and k is the ratio between (e_0^* - e_A) and (e_s^* - e_A), as shown in Figure 3.1. Despite T_0 driving the sensible heat flux, the comprehensive dry-wet signature of the underlying surface due to soil moisture variations is directly reflected in T_R. Thus, T_R in the

denominator is directly related to the surface moisture availability (*M*). In Equation 3.16, T_{0D} computation is challenging because both e_0 and s_1 are unknown. By decomposing the aerodynamic equation of λE, T_{0D} can be expressed as follows

$$\lambda E = \frac{\rho c_p}{\gamma} g_A (e_0 - e_A) = \frac{\rho c_p}{\gamma} g_A s_1 (T_{0D} - T_D) \tag{3.17}$$

$$T_{0D} = T_D + \frac{\gamma \lambda E}{\rho c_p g_A s_1} \tag{3.18}$$

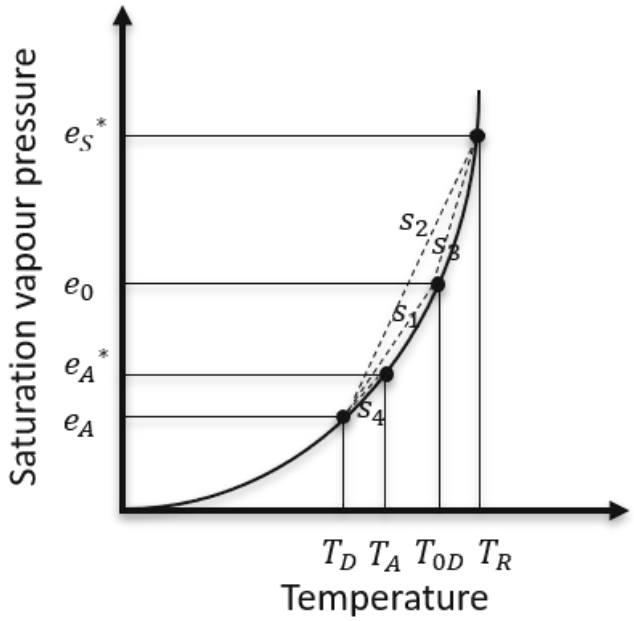

Figure 3.3. Schematic representation

An iterative method is applied to solve the equations because λE and e_0^*, e_0, α and *M* are entangled. An initial value of α is assigned as 1.26 and initial estimates of e_0^*, e_0 are obtained from T_R and *M* as

$$e_0{}^* = 6.13753 e^{\frac{17.27 T_R}{T_R + 237.3}} \tag{3.19}$$

$$e_0 = e_A + M(e_0{}^* - e_A). \tag{3.20}$$

M is initialized by assuming $e_0^* = e_s^*$, i.e. *k* in Equation 3.16 equals 1, expressed as follows

$$M = \frac{s_1 (T_{0D} - T_D)}{s_2 (T_R - T_D)}. \tag{3.21}$$

To obtain T_{0D}, s_1 and s_3 can be expressed as follows

$$s_1 = \frac{e_0 - e_A}{T_{0D} - T_D} \tag{3.22}$$

$$s_3 = \frac{e_s^* - e_0}{T_R - T_{0D}}. \tag{3.23}$$

Combing equations 3.22 and 3.23, T_{0D} can be expressed as

$$T_{0D} = \frac{e_s^* - e_A - s_3 T_R + s_1 T_D}{s_1 - s_3}. \tag{3.24}$$

The slopes s_1 and s_3 can be expressed as

$$s = 4098 \frac{6.13753 e^{\frac{17.27T}{T+237.3}}}{(T + 237.3)^2} \tag{3.25}$$

where T is set to T_D and T_R for s_1 and s_3, respectively. With the initial estimates of e_0^*, e_0, α and M, g_A, g_C and λE can be calculated. Then e_0^*, e_0, α and M are updated, λE is recalculated. The iteration continues until the convergence of λE is achieved.

By considering the hysteresis between T_R, D_A and λE, the surface moisture availability M can be expressed as

$$M = \frac{\gamma s_1 (T_{0D} - T_D)}{s_3 (T_R - T_{0D}) s + \gamma s_4 (T_A - T_D)} \tag{3.26}$$

Hysteresis occurs because the capacity of the soil and vegetation to supply moisture to the atmosphere is larger in the morning than in the afternoon (Boegh et al. 1999). As such, two equations are used for estimating M in STIC depending on the occurrence of hysteresis. It is assumed that equation 3.16 is used to indicate surface wetness that controls the evapotranspiration from the upper few centimetres of the surface, whereas equation 3.26 is used to indicate the root-zone wetness that controls the evapotranspiration under strong hysteretic conditions between λE, R_N, T_R and D_A.

3.3. Partitioning λE into wet evaporation and transpiration

The terrestrial latent heat flux is an aggregate of both transpiration (λE_T) and evaporation (λE_E, sum of soil evaporation and interception evaporation from the canopy). During rain events, the land surface becomes wet and λE tends to approach the potential evaporation (λE^*), while surface drying after rainfall causes λE to approach the potential transpiration rate (λE_T^*) in the presence of vegetation, or zero without any vegetation. Hence,

λE at any time is a mixture of these two end-member conditions depending on the surface moisture availability, expressed as follows:

$$\lambda E = \lambda E_E + \lambda E_T = M\lambda E^* + (1 - M)\lambda {E_T}^* \quad (3.27)$$

After estimating g_A, λE^* is estimated according to the Penman equation and λE_T is estimated as the residual of equation 3.27.

3.4. Input and output parameters for the STIC model

The input variables used for running the STIC model are listed in Table 3.1. The LST and emissivity are retrieved from ECOSTRESS L2 LST&E data. The land surface properties for example albedo and fractional vegetation coverage (FVC) are obtained from the Copernicus Global Land Service (CGLS, https://land.copernicus.eu/global/index.html). The meteorological data are obtained from the ERA5 reanalysis data (https://cds.climate.copernicus.eu/cdsapp#!/search?type=dataset). All these CGLS and ERA5 data are spatially and temporally interpolated to match the ECOSTRESS LST&E data.

Table 3.1. Input parameters for the STIC model

Data	Purpose	Source	Spatial resolution	Temporal resolution
LST	R_N, T_R	ECOSTRESS	~70 m	daily
emissivity (ε_w)	R_N	ECOSTRESS	~70 m	daily
Black sky and white sky albedo (α_{bs}, α_{ws})	α_{sw}, R_N	CGLS	1 km	10-day
FVC	surface condition	CGLS	300 m	10-day
shortwave direct radiation (R_{Sdir})	α_{sw}	ERA5	0.25°	1 hour
shortwave global radiation (R_S)	R_N	ERA5	0.25°	1 hour
air temperature (T_A)	lower boundary condition	ERA5	0.25°	1 hour
atmosphere vapour pressure (e_A) or Dewpoint temperature (T_D)	lower boundary condition	ERA5	0.25°	1 hour

The outputs from the STIC model include the total ET, partitioned evaporation components (transpiration and evaporation) and net available energy at both instantaneous and daily scale.

3.5. STIC ET quality control

The STIC ET quality depends on the LST and ancillary data used in the calculation. To control the quality of the ET estimates, only LST estimates with the highest accuracy after strict cloud screening are used in the model.

4. Surface Energy Balance System (SEBS) model

The one-source SEBS model was proposed by Su (2002) which also includes sub-models for the roughness length of heat as well as momentum transfer and a formulation for the determination of the evaporative fraction on the basis of energy balance at limiting cases. The generalized flowchart for estimating λE through SEBS model is given below.

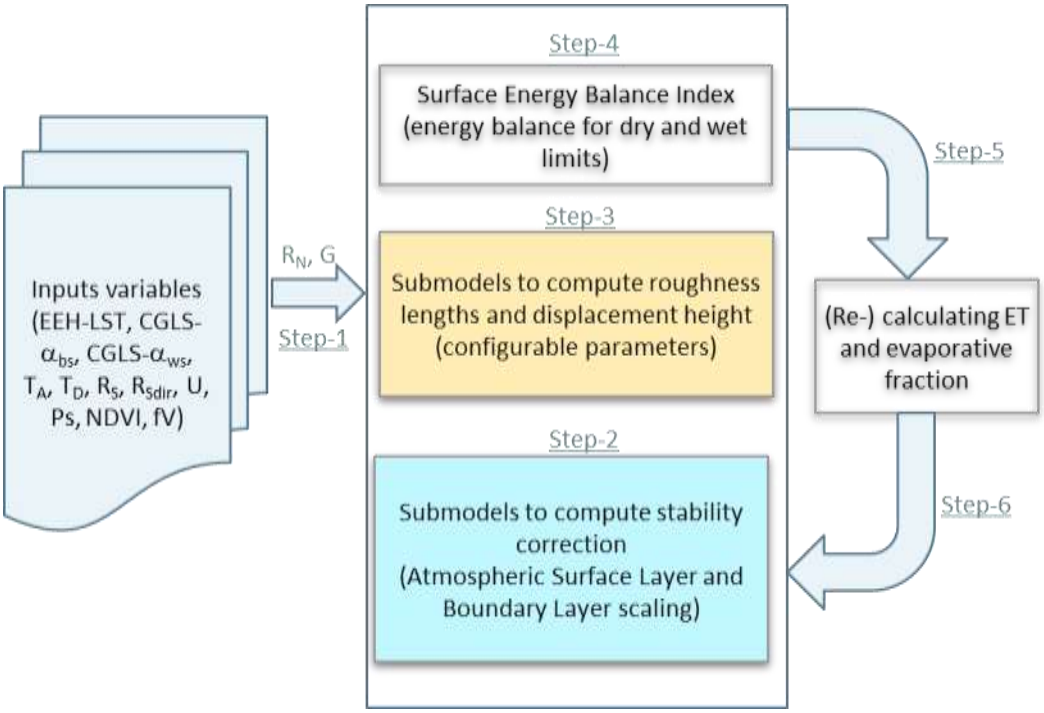

Figure 4.1. Generalized diagram of SEBS, showing different sub-models for computing surface energy balance, roughness lengths for heat and momentum transfer (yellow box), and corrections for atmospheric stability (blue box).

4.1. Surface energy balance terms

In order to derive the sensible and latent heat fluxes, the similarity theory is used. In the Atmospheric Surface Layer (ASL) similarity relationship, the profiles of the mean wind speed u and the mean temperature $\theta_0 - \theta_a$ can be expressed as follows:

$$u = \frac{u_*}{k}[\ln\left(\frac{z-d_0}{z_{0m}}\right) - \Psi_m\left(\frac{z-d_0}{L}\right) + \Psi_m(\frac{z_{0m}}{L})] \quad (4.1)$$

$$\theta_0 - \theta_a = \frac{H}{k u_* \rho c_p}[\ln\left(\frac{z-d_0}{z_{0h}}\right) - \Psi_h\left(\frac{z-d_0}{L}\right) + \Psi_h(\frac{z_{0h}}{L})] \quad (4.2)$$

where z is the height above the surface (m), $u^* = (\tau_0/\rho)^{1/2}$ is the friction velocity (m s^{-1}), τ_0 is the surface shear stress (kg m^{-1} s^{-2}), ρ is the density of air (kg m^{-3}), k = 0.4 is von Karman's

constant, d_0 is the zero plane displacement height (m), z_{0m} is the roughness height for momentum transfer (m), θ_0 is the potential temperature at the surface (°C), θ_a is the potential air temperature (°C)at height z, z_{0h} is the scalar roughness height for heat transfer (m), ψ_m and ψ_h are the stability correction functions for momentum and sensible heat transfer respectively. L is the Obukhov length, which is defined as follows.

$$L = -\frac{\rho c_p {u_*}^3 \theta_v}{kgH} \tag{4.3}$$

where g is the acceleration due to gravity (m s^{-2}) and θ_v is the potential virtual temperature near the surface.

The friction velocity, the sensible heat flux and the Obukhov stability length are obtained by solving the system of non-linear equations 4.1 – 4.3. Derivation of the sensible heat flux using the above equations requires only the wind speed and temperature at the reference height as well as the surface temperature and is independent of other surface energy balance terms.

4.2. An extended model for the roughness length for heat transfer

The relationship between the scalar roughness height for heat transfer z_{0h} and the roughness height for momentum z_{0m} can be expressed as follows:

$$z_{0h} = z_{0m}/\exp\left(kB^{-1}\right) \tag{4.4}$$

where B^{-1} is the inverse Stanton number, a dimensionless heat transfer coefficient. To estimate the kB^{-1} value, an extended model of Su et al. (2001) is developed as below

$$kB^{-1} = \frac{kc_d}{4c_t \frac{u_*}{u(h)}\left(1 - e^{-n_{ec}/2}\right)} {f_c}^2 + 2f_c f_s \frac{k.\frac{u_*}{u(h)}.z_{0m}/h}{{c_t}^*} + kB_s{}^{-1} {f_s}^2 \tag{4.5}$$

where f_c is the fractional canopy coverage and f_s is its complement, $u(h)$ is the horizontal wind speed at the top of canopy, c_t is the heat transfer coefficient of the leaf ($0.005N \le c_t \le 0.075N$ for most cases, N is number of sides of a leaf to participate in heat exchange), the heat transfer coefficient of the soil is given by ${c_t}^* = \mathrm{Pr}^{-2/3}\mathrm{Re}_*^{-1/2}$, where Pr is the Prandtl number and Re_* is the roughness Reynolds number, n_{ec} is the within-canopy wind speed profile extinction coefficient, calculated as follows:

$$n_{ec} = \frac{c_d LAI}{2{u_*}^2/u(h)^2} \tag{4.6}$$

where c_d is the drag coefficient of the foliage elements assumed to take the value of 0.2, *LAI* is the one-sided leaf area index defined for the total area.

In Equation 4.5, the first term follows the full canopy model, the second term describes the interaction between vegetation and bare soil surface, while the third term is for a bare soil surface. A quadratic weighting based on the fractional canopy coverage is used to accommodate any situation between the full vegetation and bare soil conditions. For bare soil surface kB_s^{-1} is calculated as

$$kB_s{}^{-1} = 2.46(Re_*)^{1/4} - \ln(7.4). \tag{4.7}$$

4.3. Formulation of evaporative fraction at limiting cases

Under the extreme dry limit, the latent heat flux becomes zero due to the limitation of soil moisture and the sensible heat flux is at its maximum value. The driest limit of λE (λE_{dry}) is expressed as follows.

$$\lambda E_{dry} = R_n - G_0 - H_{dry} \equiv 0 \tag{4.8}$$

$$H_{dry} = R_n - G_0. \tag{4.9}$$

Under the wet limit, where evaporation is limited only by the available energy under the given surface and atmospheric conditions and takes place at the maximum, λE_{wet}, the sensible heat flux takes its minimum value, H_{wet}, i.e.

$$H_{wet} = R_n - G_0 - \lambda E_{wet}. \tag{4.10}$$

The relative evaporation (Λ_r) can then be expressed by scaling between the driest and wettest limits of H as follows:

$$\Lambda_r = \frac{\lambda E}{\lambda E_{wet}} = 1 - \frac{\lambda E_{wet} - \lambda E}{\lambda E_{wet}} = 1 - \frac{H - H_{wet}}{H_{dry} - H_{wet}}. \tag{4.11}$$

The actual sensible heat flux *H* defined by Equation 4.2 is constrained in the range set by the sensible heat flux at the wet limit H_{wet} and that at dry limit H_{dry}. H_{dry} is given by Equation 4.9, H_{wet} can be derived by combing Equation 4.10 and a combination equation similar to the Penman-Monteith combination equation (eq. 4.12 below)

$$\lambda E = \frac{\mathrm{s}.r_e.(R_n - G_0) + \rho c_p D_a}{r_e(\gamma + \mathrm{s}) + \gamma.r_i} \quad (4.12)$$

where r_e and r_i are the bulk aerodynamic and surface internal resistances, respectively. At the wet limit, the internal resistance is 0. Then the sensible heat flux at the wet limit is obtained from the complementary form of the PM equation as follows:

$$H_{wet} = \frac{(R_n - G_0) - \rho c_p D_a/(r_{ew}.\gamma)}{1 + s/\gamma} \quad (4.13)$$

where r_{ew} is the bulk aerodynamic resistance at the wet limit. The aerodynamic resistance can be obtained in the same way as in Equation 4.2 as follows:

$$r_{ew} = \frac{1}{ku_*}[\ln\left(\frac{z-d_0}{z_{0h}}\right) - \Psi_h\left(\frac{z-d_0}{L_w}\right) + \Psi_h(\frac{z_{0h}}{L_w})] \quad (4.14)$$

where L_w is stability length at the wet limit, expressed as follows:

$$L_w = -\frac{\rho {u_*}^3}{kg.0.61.\frac{R_n - G_0}{\lambda}}. \quad (4.15)$$

The evaporative fraction is finally given by equation 4.16 (below)

$$F_E = \frac{\lambda E}{R_n - G_0} = \frac{\Lambda_r.\lambda E_{wet}}{R_n - G_0}. \quad (4.16)$$

4.4. Input and output parameters for the SEBS model

The input parameters used for the SEBS model are listed in Table 4.1. The LST and emissivity are retrieved from ECOSTRESS L2 LST&E data. The surface biophysical properties such as albedo and fractional vegetation coverage (FVC) are obtained from the Copernicus Global Land Service (CGLS). The meteorological data are obtained from the ERA5 reanalysis data. All these CGLS and ERA5 data are spatially and temporally interpolated to match the ECOSTRESS LST&E data.

Table 4.1. Input parameters for the SEBS model

Data	Purpose	Source	Spatial resolution	Temporal resolution
LST	R_N, T_R	ECOSTRESS	~70 m	daily
emissivity	R_N	ECOSTRESS	~70 m	daily
Black sky and white sky albedo (α_{bs}, α_{ws})	α_{sw}, R_N	CGLS	1 km	10-day
Fractional vegetation cover (f_v)	G	CGLS	300 m	10-day
Leaf area index (LAI)	aerodynamic resistance	CGLS	300 m	10-day

LULC	canopy characteristics	CGLS	100 m	annual
shortwave global radiation (R_S)	R_N	ERA5	0.25°	1 hour
air temperature (T_A)	lower boundary condition	ERA5	0.25°	1 hour
atmosphere vapour pressure (e_A) or dewpoint temperature (T_D)	lower boundary condition	ERA5	0.25°	1 hour
wind speed (U)	aerodynamic resistance	ERA5	0.25°	1 hour
surface pressure (P_s)	surface coefficients	ERA5	0.25°	1 hour

The outputs from the SEBS model consist of the bulk instantaneous and daily latent heat fluxes. No actions will be taken to partition λE into transpiration and evaporation components.

5. Two-Source Energy Balance (TSEB) model

The TSEB model was first proposed by Norman et al. (1995) via hypothesizing the surface as a combination of soil and vegetation components. Through the introduction of the TSEB model, the problem of defining the extra resistance caused due to directly using the radiometric temperature instead of aerodynamic temperature in the calculation of sensible heat is bypassed. The generalized flow diagram of TSEB and different sub-models are shown in figure 5.1 below.

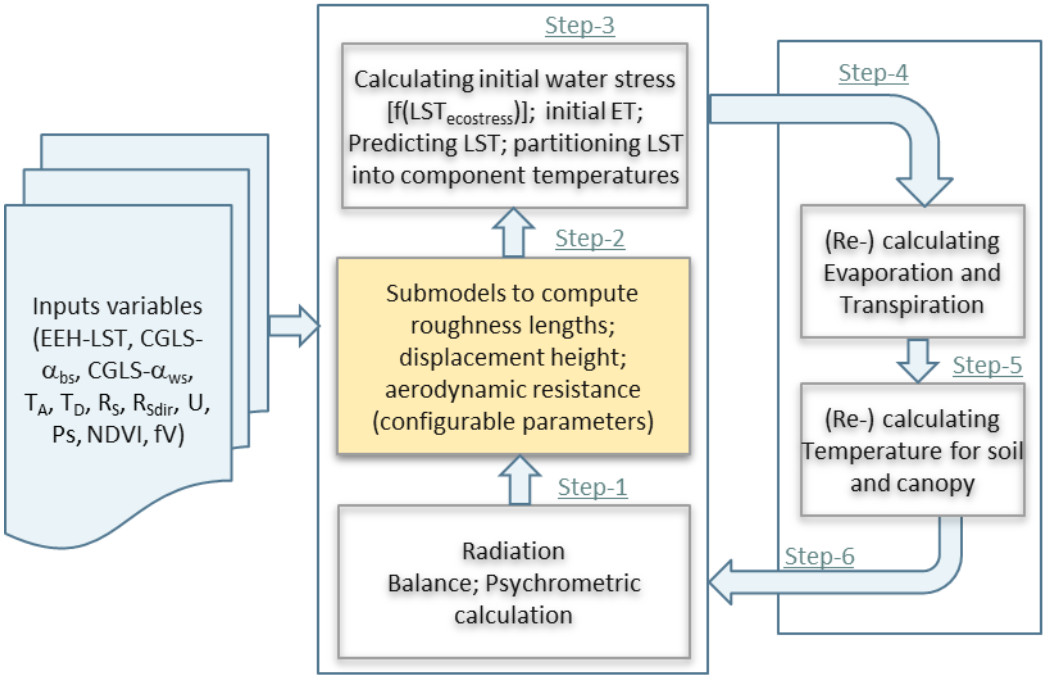

Figure 5.1. Generalized diagram of TSEB.

5.1. Radiation calculation

In the TSEB model, the satellite-derived directional radiometric surface temperature at the viewing angle ϕ ($T_R(\phi)$) is considered to be a composite of the soil surface and canopy temperatures, respectively. It is expressed as,

$$T_R(\phi) \approx [f_C(\phi){T_C}^4 + (1 - f_C(\phi)){T_S}^4]^{1/4} \quad (5.1)$$

where T_C is canopy temperature, T_S is soil surface temperature, and $f_C(\phi)$ is the fractional vegetation cover observed at the radiometer view angle. For a canopy with a spherical leaf angle distribution and leaf area index (LAI), $f_C(\phi)$ can be expressed as

$$f_C(\phi) = 1 - \exp\left(\frac{-0.5\Omega LAI}{\cos(\phi)}\right) \quad (5.2)$$

where Ω is the clumping factor, indicating the degree to which vegetation is clumped, as in row crops or shrubland canopies (Kustas and Norman 1999).

The net radiations from the individual soil and canopy components are expressed as follows:

$$L_{N,S} = \exp(-k_L LAI)\, L_{sky} + (1 - \exp(-k_L LAI))L_C - L_S \quad (5.3)$$

$$L_{N,C} = (1 - \exp(-k_L LAI))\,(L_{sky} + L_S - 2L_C) \quad (5.4)$$

$$R_{N,S} = S_{N,S} + L_{N,S} \quad (5.5)$$

$$R_{N,C} = S_{N,C} + L_{N,C} \quad (5.6)$$

Where , $R_{N,S}$ and $R_{N,C}$ are the net radiation for the soil and canopy components, k_L is the extinction coefficient (~0.95), L_{sky}, L_C and L_S are the longwave emissions from the sky, canopy and soil, respectively, which are calculated using air temperature (calculated from shelter level air temperature and vapour pressure), canopy temperature (T_C) and soil temperature (T_S), respectively. $L_{N,S}$ and $L_{N,C}$ are the net longwave radiation for the soil and canopy components, respectively, $S_{N,S}$ and $S_{N,C}$ are the net shortwave radiation for the soil and canopy components, respectively.

5.2. Energy balance calculation

Component radiometric temperatures are used to compute the surface energy balance fluxes for the canopy and soil components of the combined land surface system.

$$R_{N,S} = H_S + \lambda E_S + G \quad (5.7)$$

$$R_{N,C} = H_C + \lambda E_C \quad (5.8)$$

where H_S and H_C are soil and canopy sensible heat fluxes, respectively, λE_S and λE_C are the soil evaporation and canopy transpiration, respectively, G is the soil conduction heat flux.

By using the series resistance network to account for the interactions between the soil and vegetation canopy fluxes, the sensible heat fluxes can be expressed as follows:

$$H_S = \rho c_p \frac{T_S - T_{AC}}{R_S} \tag{5.9}$$

$$H_C = \rho c_p \frac{T_C - T_{AC}}{R_X} \tag{5.10}$$

where R_S and R_X are the aerodynamic resistance from soil surface and total boundary layer aerodynamic resistance of the complete canopy leaves, respectively, T_{AC} is the momentum aerodynamic temperature.

The total sensible heat flux $H = H_S + H_C$ can be expressed as follows:

$$H = \rho c_p \frac{T_{AC} - T_A}{R_A} \tag{5.11}$$

where T_A is the air temperature, R_A is the aerodynamic resistance to heat transfer (s/m), which is expressed as follows.

$$R_A = \frac{[\ln\left(\frac{z_U - d_0}{z_{0M}}\right) - \psi_M][\ln\left(\frac{z_T - d_0}{z_{0M}}\right) - \psi_H]}{k^2 u} \tag{5.12}$$

where d_0 is the zero-plane displacement height (m), u is the wind speed (m/s) measured at height z_U, k is von Karman's constant (~0.4), z_T is the height (m) of the T_A measurement, ψ_M and ψ_H are the Monin-Obukhov stability functions for momentum and heat, respectively, z_{0M} is the roughness length (m) for momentum transport.

For the latent heat flux from the canopy, the Priestly-Taylor formula is used to initially estimate a potential rate for λE_C

$$\lambda E_C = \alpha_{PT} f_G \frac{s}{s + \gamma} R_{N,C} \tag{5.13}$$

where α_{PT} is the Priestly-Taylor constant, with the initial value set to 1.3 and a higher value (~2) under well-watered partial canopy cover conditions in advective environments, f_G is the fraction of green vegetation, with the initial value set to 1.

The latent heat flux from the soil surface is solved as a residual in the energy balance equation

$$\lambda E_S = R_{N,S} - G - H_S \tag{5.14}$$

where G is estimated as a fraction of the net radiation at the soil surface

$$G = c_G R_{N,S} \tag{5.15}$$

where c_G is assumed to be ~0.3 based on experimental data from several sources.

5.3. Iteration of the energy partitioning

Based on the λE_C initially calculated using Equation 5.13, the initial canopy temperature T_C can be obtained as follows

$$T_c = T_a + \frac{R_{N,C} R_A}{\rho c_p}\left[1 - \alpha_{PT} f_G \frac{s}{s+\gamma}\right]. \quad (5.16)$$

The soil temperature T_S can be obtained based on Equation 5.1. Then the sensible and latent heat fluxes of soil are calculated based on the energy balance. Non-physical solutions, such as daytime condensation at the soil surface (i.e. λE_S <0), can be obtained under conditions of moisture deficiency. This occurs because the initial value of α_{PT} used for the initiation of λE_C can lead to an overestimation of transpiration in water deficit environments. If this is encountered, α_{PT} is iteratively reduced until λE_S approaches 0.

5.4. Input and output parameters for the TSEB model

The input parameters used for the TSEB model are listed in Table 5.1. The LST and emissivity are retrieved from ECOSTRESS L2 LST&E data. The surface property parameters such as albedo and fractional vegetation coverage (FVC) are obtained from the Copernicus Global Land Service (CGLS). The meteorological data are obtained from the ERA5 reanalysis data. All these CGLS and ERA5 data are spatially and temporally interpolated to match the ECOSTRESS LST&E data.

Table 5.1. Input parameters for the TSEB model

Data	Purpose	Source	Spatial resolution	Temporal resolution
LST	R_N, T_R	ECOSTRESS	~70 m	daily
emissivity	R_N	ECOSTRESS	~70 m	daily
Black sky and white sky albedo (α_{bs}, α_{ws})	α_{sw}, R_N	CGLS	1 km	10-day
Fractional vegetation cover (f_v)	G	CGLS	300 m	10-day
Leaf area index (LAI)	aerodynamic resistance	CGLS	300 m	10-day
LULC	canopy characteristics	CGLS	100 m	annual
shortwave direct radiation (R_{Sdir})	α_{sw}	CGLS	1 km	daily
shortwave global radiation (R_S)	R_N	ERA5	0.25°	1 hour
air temperature (T_A)	lower boundary condition	ERA5	0.25°	1 hour

atmosphere vapour pressure (e_A) or dewpoint temperature (T_D)	lower boundary condition	ERA5	0.25°	1 hour
wind speed (U)	aerodynamic resistance	ERA5	0.25°	1 hour
surface pressure (P_S)	surface coefficients	ERA5	0.25°	1 hour

6. Temporal upscaling from instantaneous to daily ET

The ET calculated using the ECOSTRESS LST&E products only represents the instantaneous latent heat flux for a single timestamp during the satellite overpass time. To upscale the instantaneous ET (ET_t) to daily total ET (ET_d), three methods are conventionally followed: (a) the first method uses top-of-atmosphere shortwave radiation as a scaling factor (Rs_{toa}, hereafter); (b) the second method applies surface downwelling shortwave radiation as a scaling factor (R_s); and (c) the third method applies diurnal conservation of evaporative fraction (F_E) concept. Despite all these methods have been widely used, they suffer from different limitations, as explained below in Table 6.1.

Table 6.1. A list of methods used for upscaling instantaneous to daily ET, their advantages and underlying limitations

Method	Main Equation	Advantages (A) and limitations (L)
Rs_{toa}	$\frac{ET_d}{ET_t} \cong \frac{Rs_{toa,d}}{Rs_{toa,t}}$	(A1) Simple and astronomically driven. No ancillary data is needed; (A2) Found to perform reasonably well for 8-day daily ET estimation and under water unstressed conditions when ET is driven by radiation only. (L1) This method produces substantial overestimation in daily ET in water limited ecosystems and under dynamic cloudy sky conditions.
R_s	$\frac{ET_d}{ET_t} \cong \frac{Rs_d}{Rs_t}$	(A1) Simple and dependent on shortwave radiation only; (A2) Found to perform reasonably well at the daily scale and under variable cloudiness. (L1) There is no universally agreed method to obtain daily Rs from remote sensing data and ET upscaling will be dependent on reanalysis data which could be uncertain; (L2)This method does not account the water stress effects on daily ET and produces overestimation in daily ET in water limited ecosystems.

F_E	$ET_d \approx \frac{ET_t(R_N - G)_d}{(R_N - G)_t}$ $\approx F_{E,t}A_d$	(A1) Considers daily net available energy (A_d) in the scaling equation; (A2) Found to perform reasonably well at the daily scale and relatively better than the previous two methods. (L1) There is no universally agreed method to obtain A_d from polar-orbiting remote sensing data; (L2) ET upscaling will be dependent on net radiation and ground heat flux of reanalysis data. This means in the estimation of ET_d, only instantaneous F_E from remote sensing will be used and therefore, this approach will not generate a predominant remote sensing based ET_d.

To circumvent the above-mentioned limitations, we propose a new upscaling strategy that exploits the advantages of the Rs_{toa} method and simultaneously add additional scaling constraints to capture the soil moisture-, net radiation- and air temperature-induced variations in ET_d based on different time of day and different biomes categories. According to the new method, the mathematical representation of ET_t to ET_d is as follows,

$$\frac{ET_d}{ET_t} = f_{sm} f_{T_A} f_{R_N} \frac{Rs_{toa,d}}{Rs_{toa,t}} \tag{5.1}$$

where f represents functions of different scaling factors and the subscripts refer to the respective variables, with which Rs_{toa} is constrained for converting ET_t to ET_d. These scalars are expressed as follows,

$$f_{sm} = \frac{RL_{in,t}}{RL_{out,t}} \tag{5.2}$$

$$f_{T_a} = \frac{T_{A,t}}{T_{a,max}} \tag{5.3}$$

$$f_{R_N} = \frac{R_{N,t}}{RS_{N,t} + RL_{in,t}}. \tag{5.4}$$

The inclusion of longwave radiations in f_{sm} will integrate the effects of soil moisture; the inclusion of T_a and radiation components will integrate the effects of maximum temperature stress and radiation balance on daily ET.

Acknowledgement

The research was carried out at the Luxembourg Institute of Science and Technology, under a contract with the European Space Agency.

7. Reference

Boegh, E., Soegaard, H., Hanan, N., Kabat, P., & Lesch, L. (1999). A remote sensing study of the NDVI–Ts relationship and the transpiration from sparse vegetation in the Sahel based on high-resolution satellite data. *Remote sensing of Environment, 69*, 224-240

Brutsaert, W., & Stricker, H. (1979). An advection-aridity approach to estimate actual regional evapotranspiration. *Water Resources Research, 15*, 443-450

Chen, J.M., & Liu, J. (2020). Evolution of evapotranspiration models using thermal and shortwave remote sensing data. *Remote sensing of Environment, 237*, 111594

Fisher, J.B., Lee, B., Purdy, A.J., Halverson, G.H., Dohlen, M.B., Cawse-Nicholson, K., Wang, A., Anderson, R.G., Aragon, B., & Arain, M.A. (2020). ECOSTRESS: NASA's next generation mission to measure evapotranspiration from the International Space Station. *Water Resources Research, 56*, e2019WR026058

Kustas, W.P., & Norman, J.M. (1999). Evaluation of soil and vegetation heat flux predictions using a simple two-source model with radiometric temperatures for partial canopy cover. *Agricultural and Forest Meteorology, 94*, 13-29

Mallick, K., Boegh, E., Trebs, I., Alfieri, J.G., Kustas, W.P., Prueger, J.H., Niyogi, D., Das, N., Drewry, D.T., & Hoffmann, L. (2015). Reintroducing radiometric surface temperature into the P enman-M onteith formulation. *Water Resources Research, 51*, 6214-6243

Mallick, K., Jarvis, A.J., Boegh, E., Fisher, J.B., Drewry, D.T., Tu, K.P., Hook, S.J., Hulley, G., Ardö, J., & Beringer, J. (2014). A Surface Temperature Initiated Closure (STIC) for surface energy balance fluxes. *Remote sensing of Environment, 141*, 243-261

Mallick, K., Toivonen, E., Trebs, I., Boegh, E., Cleverly, J., Eamus, D., Koivusalo, H., Drewry, D., Arndt, S.K., & Griebel, A. (2018a). Bridging Thermal Infrared Sensing and Physically-Based Evapotranspiration Modeling: From Theoretical Implementation to Validation Across an Aridity Gradient in Australian Ecosystems. *Water Resources Research, 54*, 3409-3435

Mallick, K., Trebs, I., Boegh, E., Giustarini, L., Schlerf, M., Drewry, D.T., Hoffmann, L., Randow, C.v., Kruijt, B., & Araùjo, A. (2016). Canopy-scale biophysical controls of

transpiration and evaporation in the Amazon Basin. *Hydrology and Earth System Sciences, 20*, 4237-4264

Mallick, K., Wandera, L., Bhattarai, N., Hostache, R., Kleniewska, M., & Chormanski, J. (2018b). A critical evaluation on the role of aerodynamic and canopy–surface conductance parameterization in SEB and SVAT models for simulating evapotranspiration: A case study in the upper biebrza national park wetland in poland. *Water, 10*, 1753

Monteith, J.L. (1965). Evaporation and environment. In (pp. 205-234): Cambridge University Press (CUP) Cambridge

Norman, J.M., Kustas, W.P., & Humes, K.S. (1995). Source approach for estimating soil and vegetation energy fluxes in observations of directional radiometric surface temperature. *Agricultural and Forest Meteorology, 77*, 263-293

Penman, H.L. (1948). Natural evaporation from open water, bare soil and grass. *Proceedings of the Royal Society of London. Series A. Mathematical and Physical Sciences, 193*, 120-145

Priestley, C.H.B., & Taylor, R.J. (1972). On the assessment of surface heat flux and evaporation using large-scale parameters. *Monthly weather review, 100*, 81-92

Shuttleworth, W.J., & Wallace, J.S. (1985). Evaporation from sparse crops-an energy combination theory. *Quarterly Journal of the Royal Meteorological Society, 111*, 839-855

Su, Z. (2002). The Surface Energy Balance System (SEBS) for estimation of turbulent heat fluxes. *Hydrology and Earth System Sciences, 6*, 85-100

Su, Z., Schmugge, T., Kustas, W.P., & Massman, W.J. (2001). An evaluation of two models for estimation of the roughness height for heat transfer between the land surface and the atmosphere. *Journal of applied meteorology, 40*, 1933-1951

Venturini, V., Islam, S., & Rodriguez, L. (2008). Estimation of evaporative fraction and evapotranspiration from MODIS products using a complementary based model. *Remote sensing of Environment, 112*, 132-141